BIOLOGY LETTERS

royalsocietypublishing.org/journal/rsbl

Research

Cite this article: Forni G, Nicolini F, Martelossi J, Savojardo C, Corneti S, Marrone F, Luchetti A. 2026 The elusive genomic signature of tadpole shrimps' ancient morphology. *Biol. Lett.* **22**: 20250130.
https://doi.org/10.1098/rsbl.2025.0130

Received: 10 March 2025
Accepted: 14 January 2026

Subject Category:
Evolutionary biology

Subject Areas:
evolution, molecular biology, bioinformatics

Keywords:
living fossils, morphological stasis, comparative genomics, Branchiopoda, *Daphnia*, genome alignment, gene family evolution

Authors for correspondence:
Filippo Nicolini
e-mails: fn76@leicester.ac.uk;
filippo.nicolini6@unibo.it
Andrea Luchetti
e-mail: andrea.luchetti2@unibo.it

†These authors contributed equally to the study.

Supplementary material is available online at
https://doi.org/10.6084/m9.figshare.c.8292155.

THE ROYAL SOCIETY PUBLISHING

The elusive genomic signature of tadpole shrimps' ancient morphology

Giobbe Forni[1,†], Filippo Nicolini[1,2,†], Jacopo Martelossi[1,3], Castrense Savojardo[4], Simona Corneti[1], Federico Marrone[5] and Andrea Luchetti[1]

[1]Department of Biological, Geological and Environmental Sciences, Università di Bologna, Bologna, Italy
[2]School of Biological and Biomedical Sciences, Division of Genetics and Genome Biology, University of Leicester, Leicester, UK
[3]Senckenberg Research Institute and Natural History Museum Frankfurt, Frankfurt, Germany
[4]Department of Pharmacy and Biotechnology, University of Bologna, Bologna, Italy
[5]Department of Biological, Chemical and Pharmaceutical Sciences, University of Palermo, Palermo, Italy

GF, 0000-0003-3669-8693; FN, 0000-0002-3749-3932; JM, 0000-0003-4227-0669; CS, 0000-0002-7359-0633; FM, 0000-0002-4730-0452; AL, 0000-0002-2986-721X

The tempo of evolutionary change varies widely across the tree of life, with some lineages undergoing extensive morphological diversification while others remain remarkably static. Notostraca, or tadpole shrimps, exemplify the latter, displaying minimal morphological change for hundreds of millions of years. To investigate the molecular basis of this exceptional stasis, we generated high-quality genome assemblies for *Triops granarius* and *Triops simplex*. These genomes, combined with data from 18 additional branchiopod species representing Notostraca and Onychocaudata, were employed for phylogenetic reconstruction and time estimation and support the emergence of Notostraca and their general morphology in the Devonian (approx. 390 Ma). We identified genes with significantly reduced rates of protein evolution in Notostraca compared to their more morphologically diverse sister group, Onychocaudata. Functional annotation linked these genes to morphogenesis and development, but we also detected genes with accelerated protein evolution associated with similar developmental processes. Notably, genes undergoing a decelerated evolution in their protein-coding sequences lack signatures of evolutionary constraints in their non-coding regions. In addition, sequence evolution and gene family expansion/contraction dynamics appear decoupled from the rate of protein evolution, suggesting that genes can undergo reduced evolutionary change in one aspect, but not in others. Our findings reveal a complex interplay between genomic and phenotypic evolution and suggest that morphological stasis is maintained by multiple molecular processes rather than by a single, overarching mechanism.

1. Introduction

The pace of evolutionary change is uneven across the different branches of the tree of life [1] and is affected by several factors, including broad-scale phenomena that can affect multiple lineages co-existing at the same time [2,3]. For example, mass extinctions are frequently followed by pronounced shifts in body size, with surviving taxa generally exhibiting smaller sizes than their predecessors [4]. Nevertheless, evolutionary rate variation is also extensive across contemporary lineages [5–7]. While many examples of uneven rate of change exist for molecular or life history traits [8,9], morphological evolution often provides striking examples of pronounced rate heterogeneity. In certain cases, reduced rates of change regard specific anatomical traits [10]; yet in some instances, stasis pervades multiple aspects. Examples of static morphologies can be found across the tree of life, especially where fossil records

are available. Horseshoe crabs of the genus *Limulus* [11], coelacanths [12] and *Ginkgo* species [13] are some prominent examples of clades with various degrees of morphological conservatism. They have been appointed several times as 'living fossils', although this status and terminology are debated and considered controversial by many [11,12,14,15]. In some instances, analyses of molecular evolutionary rates in a handful of 'living fossil' lineages have suggested that these clades exhibit slower rates of genomic change, aligning with their phenotypic stasis [16,17].

Among the numerous cases of morphological conservatism, Notostraca—commonly known as tadpole shrimps—stands as an iconic example. Fossils from the Upper Carboniferous (approx. 300 million years ago (Ma)) indicate that the fundamental body plan of Notostraca may have remained virtually unaltered over geological timescales [15,18,19]. Despite exhibiting substitution rates that are comparable to—or only marginally lower than—those of their sister clade Onychocaudata, Notostraca species show a dynamic genome evolution, with a rapid turnover in gene family expansions and contractions, as well as in the transposable elements (TEs) composition [20,21]. This suggests the absence of a molecular counterpart to the morphological stasis often associated with so-called living fossils [22], leaving the genomic basis for Notostraca's striking conservatism elusive. These findings raise a critical question about the mechanisms constraining phenotypic evolution: can conserved morphology be linked to a handful of conserved genes?

Here, we use a phylogenomic framework—augmented with new genomes for *Triops granarius* (Lucas, 1864) and *Triops simplex* (Ghigi, 1921)—to test: (i) whether the subset of genes that exhibit decelerated protein-sequence evolution in Notostraca relative to the sister clade Onychocaudata is enriched for morphogenesis and developmental functions; and (ii) whether these genes also show decelerated changes in complementary metrics, such as conservation in non-coding regions and reduced gene-family turnover. Our findings highlight the complexity of linking genomic dynamics to morphological evolution, and that genes can undergo a slow evolutionary change in one aspect, but not in others.

2. Results and discussion

(a) New genome assemblies, orthology and time tree inference

Currently, genome assemblies are available for eight species within Notostraca: five belonging to the *Lepidurus* genus, while only two to its sister *Triops*. To achieve a more balanced taxonomic representation of the order, we produced new genome assemblies and annotations for *T. granarius* and *T. simplex*. Assembly lengths resulted in 86.69 and 97.86 Mb (electronic supplementary material, table S1), respectively, corresponding to a theoretical genome coverage of 88X and 75X. Assembled genomes were checked for completeness using the arthropods' gene set of BUSCO and resulted in 96.0% and 95.5% of complete genes, respectively (electronic supplementary material, table S1). Gene predictions successfully annotated 11 994 and 12 835 genes, whereas 8.75% and 10.82% of the genomes were composed of repetitive elements (electronic supplementary material, table S2).

The final dataset for orthology inference encompassed the proteomes of 10 Notostraca samples (five species of the genus *Lepidurus* and four species of the genus *Triops*, with *Triops cancriformis* (Bosc, 1801) represented by both a bisexual (ESP) and a parthenogenetic (ITA) lineage; [20,23]), seven Anomophoda (six *Daphnia* species and *Chydorus sphaericus* (O.F. Müller, 1776); [24–29]), two Spinicaudata (*Leptestheria dahalacensis* (Rüppell, 1837) and *Eulimnadia texana* (Packard, 1871); [20,30]) and one Anostraca outgroup (*Artemia franciscana* (Kellog, 1906)). All assemblies included in the dataset have a BUSCO completeness higher than 95% (except *A. franciscana* with 89.6%; electronic supplementary material, table S1).

The orthology inference among the proteomes of the 20 species clustered 93.3% of genes in orthogroups (OGs), of which 5.5% were species-specific. In total, 425 OGs contained single-copy genes for all taxa and reconstructed a maximum likelihood phylogenetic tree with maximum support for all nodes, except for the one leading to the group *Lepidurus apus apus* (Linnaeus, 1758), *Lepidurus cf. couesii* (Packard, 1875) and *Lepidurus arcticus* (Pallas, 1793), which is scored 61. Major phylogenetic relationships within Branchiopoda have been recovered, with Notostraca forming a monophyletic group in a sister relationship to Onychocaudata (figure 1*a*). Divergence time estimates are coherent with literature and the fossil record ([32]; electronic supplementary material, table S3), and place the emergence of crown Phyllopoda (in this study represented by Notostraca + Onychocaudata) in the Ordovician (approx. 450 Ma), of *L. dahalacensis* + *E. texana* in the Cretaceous (approx. 140 Ma) and of crown Anomopoda (in this study represented by *C. sphaericus* + *Daphnia* spp.) in the Jurassic (approx. 150 Ma; [33–38]).

(b) Protein rate of evolution analysis

Considering that we employed an *ab-initio*-based approach for predictions of CDSs and proteins, without incorporating RNA-seq evidence from the same species, we checked for the possible impact of spurious annotations, which could be relevant and potentially have affected molecular evolutionary analyses [39,40]. Particularly, we checked for: (i) differences in general gene statistics; (ii) differences in BUSCO scores; and (iii) the influence of annotation approaches on predicted protein lengths. We found (i) no consistent deviation of gene, intron and exon lengths between Notostraca and the other species included (electronic supplementary material, figure S1), as well as (ii) no changes in BUSCO statistics at the genome (before annotation) and the proteome levels (after annotation; electronic supplementary material, table S1). For genes included in the molecular evolutionary analyses (see below), we fitted a linear mixed model including OGs (genes) and species (annotation method—Notostraca all share the same *ab-initio* annotation pipeline; see §4) as random effects. Most of the variation in protein length was explained by OGs (variance = 220,154), whereas (iii) the effect of the annotation type was minimal (Notostraca proteins

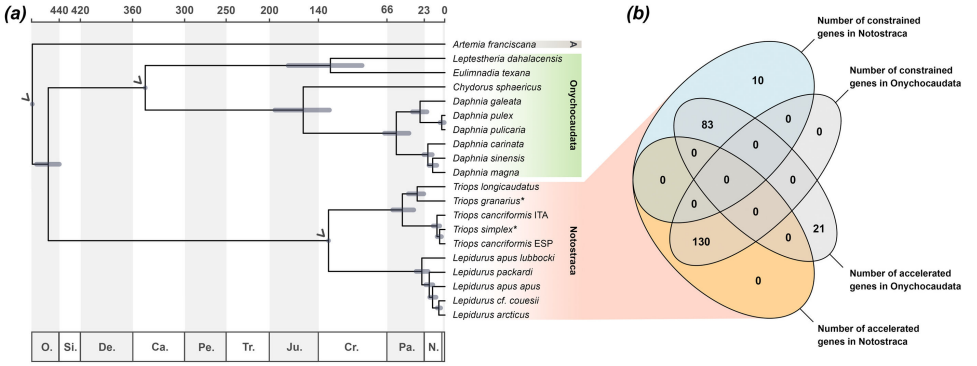

(c)

ID	Constrained gene terms	p-value	Significative/Expected
GO:0007249	I-kappaB kinase/NF-kappaB signaling	0.00217	11.54
GO:0006357	regulation of transcription by RNA polymerase II	0.00384	2.37
GO:0006470	protein dephosphorylation	0.00784	5.06
GO:0006355	regulation of transcription, DNA-templated	0.00819	1.93
GO:1903506	regulation of nucleic acid-templated transcription	0.00819	1.93
GO:2001141	regulation of RNA biosynthetic process	0.00819	1.93
GO:0006366	transcription by RNA polymerase II	0.00832	2.15
GO:0060271	cilium assembly	0.00954	4.76
GO:0007018	microtubule-based movement	0.01198	4.44
GO:0044782	cilium organization	0.01251	4.4
GO:0030030	cell projection organization	0.01277	2.76
GO:0042326	negative regulation of phosphorylation	0.01546	5.66
GO:0044260	cellular macromolecule metabolic process	0.01682	1.34
GO:0044419	interspecies interaction between organism	0.01728	3.29
GO:0006351	transcription, DNA-templated	0.01793	1.77
GO:0097659	nucleic acid-templated transcription	0.01793	1.77
GO:0120031	plasma membrane bounded cell projection assembly	0.01799	3.96
GO:0002009	morphogenesis of an epithelium	0.01831	5.36
GO:0032774	RNA biosynthetic process	0.01834	1.76
GO:0051252	regulation of RNA metabolic process	0.02193	1.72
GO:0016311	dephosphorylation	0.02236	3.7
GO:0030031	cell projection assembly	0.02236	3.7
GO:0060429	epithelium development	0.02236	2.7
GO:0010563	negative regulation of phosphorus metabolism	0.02254	4.92
GO:0045936	negative regulation of phosphate metabolism	0.02254	4.92
GO:0000280	nuclear division	0.02315	3.67
GO:0048729	tissue morphogenesis	0.02604	4.69
GO:0120036	plasma membrane bounded cell projection assembly	0.02878	2.56
GO:0009888	tissue development	0.02971	2.86
GO:0051171	regulation of nitrogen compound metabolism	0.02985	1.53

0 0.025 0.05

(d)

ID	Accelerated gene terms	p-value	Significative/Expected
GO:0010466	negative regulation of peptidase activity	0.0024	10.71
GO:0006397	mRNA processing	0.0024	2.86
GO:0016071	mRNA metabolic process	0.0029	2.48
GO:0097193	intrinsic apoptotic signaling pathway	0.0072	7.32
GO:0050684	regulation of mRNA processing	0.0077	5.06
GO:0051346	negative regulation of hydrolase activity	0.0082	7.14
GO:0045861	negative regulation of proteolysis	0.0129	6
GO:0006406	mRNA export from nucleus	0.0157	5.66
GO:0071427	ribonucleoprotein complex export from nucleus	0.0157	5.66
GO:0097190	apoptotic signaling pathway	0.0181	3.96
GO:1902532	negative regulation of intracellular signal transduction	0.0181	3.96
GO:0048024	regulation of mRNA splicing, via spliceosome	0.0188	5.26
GO:0019752	carboxylic acid metabolic process	0.0214	1.99
GO:0043436	oxoacid metabolic process	0.0249	1.94
GO:0052547	regulation of peptidase activity	0.0279	4.55
GO:0044281	small molecule metabolic process	0.0283	1.63
GO:0006520	cellular amino acid metabolic process	0.0283	2.36
GO:0051028	mRNA transport	0.03	4.41
GO:0000375	RNA splicing, via transesterification reaction	0.0376	2.41
GO:0000377	RNA splicing, via transesterification reaction	0.0376	2.41
GO:0000398	mRNA splicing, via spliceosome	0.0376	2.41
GO:0006605	protein targeting	0.0394	3.1
GO:1903311	regulation of mRNA metabolic process	0.0394	3.1
GO:0071166	ribonucleoprotein complex localization	0.0415	3.9
GO:0071426	ribonucleoprotein complex export from nucleus	0.0415	3.9
GO:0006396	RNA processing	0.042	1.65
GO:0031503	protein-containing complex localization	0.0431	3.01
GO:1901605	alpha-amino acid metabolic process	0.0437	2.59
GO:0043484	regulation of RNA splicing	0.044	3.8
GO:0071417	cellular response to organonitrogen compound	0.044	3.8

0 0.025 0.05

Figure 1. (*a*) Genome-scale divergence time estimate of the Branchiopoda species analysed in this work. Bootstrap values are 100 for all nodes except for the one leading to *Lepidurus apus apus*, *Lepidurus couesii* and *Lepidurus arcticus* [31]. Age confidence intervals (CIs) as computed by 100 LSD2 replicates are shown for each node; arrowheads indicate calibration nodes. Genomes sequenced in this work are marked with an asterisk next to the tip name. A: Anostraca. (*b*) Venn graph showing the number and overlaps of genes found to have undergone convergent protein rate of evolution in Notostraca (displaying a more static morphology) and Onychocaudata (displaying a higher morphological disparity). Genes that are constrained in Notostraca (i.e. showing a decelerated rate of protein evolution) are shown in blue, while genes accelerated in Notostraca (i.e. showing a higher rate of protein evolution) are shown in orange. Constrained and accelerated genes in Onychocaudata are shown in grey. The number of overlapping genes in each group is shown in the corresponding intersections. (*c,d*) Enriched biological-process Gene Ontology (GO) terms associated with genes having convergent protein rate of evolution in Notostraca. Only the top 30 enriched terms are shown. *p*-Values for each term are shown using a colour gradient (colour keys below each panel), while the 'significant/expected' column indicates the ratio between observed and expected terms in our genes of interest. Bars are proportional to ratio values. Colours as in panel (*b*). A comprehensive list of enriched terms is available in electronic supplementary material, table S5.

are 19.73 amino acids longer, on average) and not significant ($p = 0.199$). Summary statistics of Notostraca were comparable to those of Onychocaudata, indicating that our annotations are reliable despite the lack of transcriptomic evidence. Additionally, considering that comparative molecular evolution analyses were restricted only to the genes that are shared among Notostraca and Onychocaudata (see below), we excluded any potential misprediction that could appear as clade-specific genes and, therefore, with highly divergent sequences [40].

A convergent evolutionary rate analysis was used to assess whether genes with significantly decelerated protein evolutionary rates are linked to morphological evolution. This analysis tests, for each OG, whether branches sharing a focal trait—here, Notostraca's morphological stasis—exhibit parallel shifts in their rate of sequence evolution compared to the rest of the tree. TRACCER computes such shifts by firstly normalizing per-branch rates against genome-wide expectations, and then by assessing significance via permutation of trait labels on the tree. Negative scores correspond to convergent rate deceleration (constraint) in the focal clade, while positive scores to convergent acceleration. Of the 7470 OGs analysed, with Notostraca as the focal clade, 222 showed convergent evolutionary rate shifts in the clade. Specifically, 130 were categorized as accelerated and 93 as constrained (figure 1*b*). We then performed the same analysis using Onychocaudata as the focal clade to assess whether the evolutionary patterns observed in Notostraca were exclusive to the clade or the results of shared life-history traits. This analysis resulted in 234 OGs in Onychocaudata with convergent shifts in the rates of sequence evolution: 104 were accelerated and 130 were constrained. It is interesting to note that most genes found to be accelerated in one clade were found to be constrained in the other, and *vice versa*: that is, 89% of the genes constrained in Notostraca are accelerated in Onychocaudata, and 100% of the genes constrained in Onychocaudata are accelerated in Notostraca (figure 1*b*). This pattern might reflect

lineage-specific evolutionary paths that shaped the contrasting morphological diversity of the two clades. However, a solid and clear explanation would require a more in-depth knowledge of the identities and functions of genes in Branchiopoda.

Notostraca constrained OGs are enriched for several terms, with some of them associated with morphological development (e.g. epithelium development (GO:0048856) and tissue morphogenesis (GO:0048729); figure 1*c*; electronic supplementary material, table S5). Conversely, accelerated OGs lack any evident connection to development and morphological conservatism, as they are associated with the regulation of transcription, and the metabolism of amino acids and proteins (figure 1*d*; electronic supplementary material, table S5).

A more specific characterization of the genes associated with the Gene Ontology (GO) term 'developmental process' (GO:0032502) found 822 genes among those analysed, of which nine were constrained and 12 accelerated in Notostraca. Interestingly, a functional characterization of both constrained and accelerated genes revealed similar patterns, with homologues of genes involved in key roles in morphological development, despite their contrasting evolutionary rates (electronic supplementary material, table S5).

(c) Whole genome alignment and prediction of discrete conserved elements

To understand whether Notostraca genes identified as constrained at the protein level are also characterized by a higher conservation of their non-coding regions (introns and UTRs) compared to accelerated genes, we performed a whole genome alignment (WGA) of all Notostraca genomes and built a null model of sequences evolution using 489 582 bases corresponding to ancestral repeats, similarly to [41]. We then used this model to identify discrete conserved elements (CEs) on the chromosome-scale genome of *Lepidurus packardi*, focusing on genomic regions on which at least six species could align, thus ensuring to consider at least one species from both *Lepidurus* and *Triops*. Overall, between 45% and 65% of Notostraca genomes were successfully aligned with Progressive Cactus on *L. packardi* scaffolds, with higher rates on congeneric species, as expected (electronic supplementary material, table S6). Of the 7470 OGs considered in evolutionary rate analyses, 6524 have an orthologue gene in *L. packardi*. Of these, 95% of their exons, 81% of their introns, 62% of their 3′-, and 75% of 5′-UTR regions are covered for at least 75% of their length by cross-genus alignable regions, and were therefore considered for CEs comparison. Interestingly, we found that the different rates of protein evolution identified by TRACCER are also reflected at the nucleotide level, with constrained genes showing a higher percentage of CEs compared to the accelerated ones along their exons (two tails Wilcoxon rank sum test; $p = 0.01471$; figure 2*a*). On the other hand, despite the presence of CEs in both introns and UTR regions—approximated to 250 bp gene-flanking regions—we did not find any trace of higher nucleotide conservation (two tails Wilcoxon rank sum test; $p > 0.05$; figure 2*a*). The relatively high fragmentation did not allow us to properly test for the degree of conservation along enhancers and promoters. Highly conserved regulatory sequences are frequently associated with genes that play key roles in development, and with genes exhibiting slow rates of evolution in their protein-coding regions (PCRs; [42–44]). However, changes in enhancer and promoter sequences can evolve rapidly and lead to significant regulatory variation, even when the corresponding PCRs remain conserved [45–47].

(d) Gene copy number dynamics

Genes undergoing accelerated or constrained rates of protein sequence evolution were also tested to assess whether they show similar patterns in their copy number dynamics. The evolution of gene copy numbers in our dataset is best described by the CAFE model implementing two different gene family turnover levels (λ), one for Notostraca and one for all the other species (likelihood ratio of −142; electronic supplementary material, figure S2). Particularly, the rate of gene family turnover appears 1.2 times higher in Notostraca ($\lambda = 1.00501 \times 10^{-3}$) than in other branchiopods ($\lambda = 8.04632 \times 10^{-4}$), confirming previous observations [20]. Theoretical models in evolutionary genomics suggest that genes experiencing lower sequence constraints (evolving at faster rates) should also be subject to fewer constraints on copy number. Empirical studies have consistently supported this hypothesis across diverse taxa [48–51]. However, our findings in Notostraca do not align with this broadly observed pattern (figure 2*b*), as no significant difference in the net gene copy number variation was detected between accelerated and decelerated genes. Hence, a strong decoupling of gene copy number dynamics from coding sequences evolution rates is observed in both groups (figure 2*b*).

3. Conclusions

Our study provides new insights into the molecular basis of morphological conservatism in Notostraca and reveals a complex interplay between genomic and phenotypic evolutionary rates. We identified developmental genes with markedly decelerated rates of protein evolution that likely contribute to the morphological stability of this lineage. Yet, we also found that other genes involved in similar developmental processes evolve rapidly, suggesting that stasis and change can coexist within the same developmental framework. The decoupling between morphological and molecular evolution observed in Notostraca aligns with contemporary views on so-called 'living fossils' [52]. While these species appear to have remained morphologically and ecologically static over time [18,19], their development and physiology evolved at a different pace [53,54]. Furthermore, the very notion of morphological stasis in 'living fossils' has been repeatedly challenged (e.g. [15,55]). Although direct genotype–phenotype associations have been demonstrated for certain traits in specific systems (e.g. [56]), such clear correspondences are often absent in phenotypes shaped by extensive networks of interacting genes [57,58]. Our results therefore suggest that the

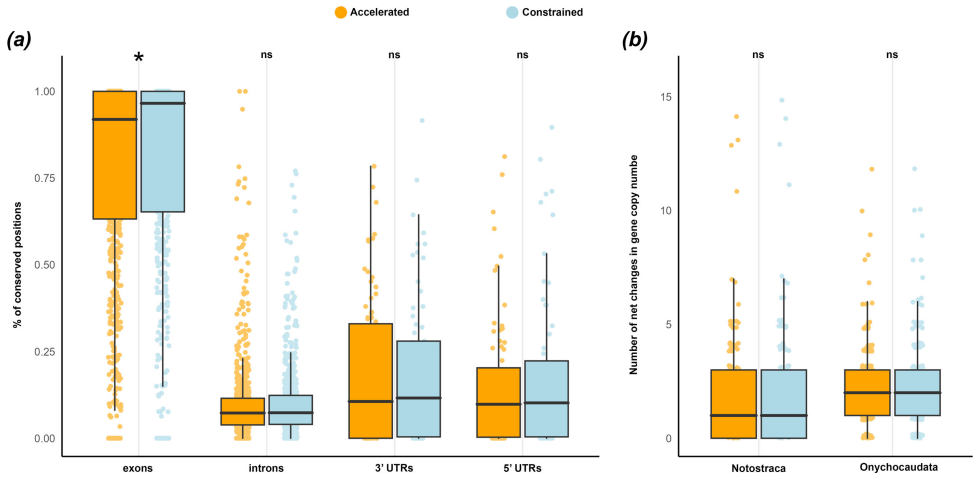

Figure 2. (*a*) Percentage of conserved nucleotide positions in exons, introns and UTR regions of *Lepidurus packardi* orthologues identified as accelerated and constrained during Notostraca evolution. (*b*) Number of net changes in gene copy number between accelerated and constrained genes in Notostraca and Onychocaudata. Significant Wilcoxon test results are shown at the top of the plot (*$p < 0.05$). Colours as in figure 1.

morphological conservatism of Notostraca stems from the interplay of multiple processes, rather than a single overarching mechanism.

4. Material and methods

(a) Genome sequencing and annotation

For the two species *T. granarius* (collected in Mongolia, Lat.: 47.072500N; Lon.: 105.841111E; [59]) and *T. simplex* (collected in Tunisia, Lat.: 35.799165N; Lon.: 10.147774E; [60]), total DNA was extracted from individual specimens using the E.Z.N.A.® Insect DNA Isolation Kit (Omega Bio-Tek) following gut removal. Whole genome sequencing was carried out on an Illumina platform (paired-end, 2 × 150 bp; insert size = 350 bp). Reads were deposited under bioprojects PRJNA1227130 (*T. granarius*) and PRJNA1227002 (*T. simplex*). Quality trimming and Illumina adapter removal were conducted using Trimmomatic v.0.39 [61], requiring a minimum quality score of 20 and a minimum read length of 30 bp. Assembly was performed using ABySS v.1.5.8 [31] with default parameters; optimal k-mer sizes (32–128 bp) were selected based on N50 statistics, considering only scaffolds longer than 1000 bp. Redundans v.0.14a [62] was used for redundancy reduction, short-read scaffolding and gap closing. BlobTools2 [63] assessed contaminants through BLAST against the NCBI nt database and taxonomic annotation at the phylum level. Minimap2 [64] aligned short reads to the assembly to calculate coverage and mapping statistics, with contaminant reads removed and re-assembled. Genome completeness was evaluated using BUSCO v.5 [65] on the Arthropoda orthologue set (n = 1,013) both on the genome assembly and on the predicted proteomes.

TEs were mined from the 10 Notostraca genomes using RepeatModeler2 [66] with the LTR-pipeline extension. The raw repeat libraries were then subjected to automatic refinement via MCHelper [67] in fully automatic mode. Each resulting TE library was then re-classified using the RepeatClassifier module of RepeatModeler2 based on DFAM (Version) and RepBase (Version) reference sequences. TEs were annotated in each genome with its respective TE library with RepeatMasker [68] in sensitive mode. After repeat masking, protein-coding genes were predicted using Augustus v.2.5 [69] as described in [21,23], with gene models from *Lepidurus apus lubbocki* (Brauer, 1873) and *L. arcticus*. Briefly, to generate reliable training sets, initial gene loci were predicted using the existing Augustus gene model for *Daphnia magna* (Straus, 1820) [23]. The resulting sequences were then aligned against the *D. magna* proteome using BLASTP (e-value <1e−4) to identify high-confidence homologues (>90% identity and >70% coverage) for both sequences. From these, 500 non-redundant loci (similarity <30%) were selected per species to train Augustus, yielding optimized *Lepidurus*-specific models for final *ab-initio* gene prediction [23].

(b) Orthology and divergence time estimation

Protein sequences for each species were used as input for OrthoFinder v.2.4.1 [70] to reconstruct OGs. OGs were aligned using MAFFT v.7.520 [71] with default parameters and trimmed using trimAl v.1.4.rev15 [72] with the heuristic selection of trimming method (--automated1). OrthoFinder single-copy OGs were used to infer the species tree with branch length estimations. IQ-TREE v.2.2.6 [73] was employed to run three independent maximum likelihood partitioned analyses on trimmed alignment, with automatic model selection as implemented by ModelFinder [74] and partition merging. Branch statistical supports were obtained with 1000 ultrafast bootstrap replicates [75]. The timetree was calibrated using LSD2 as implemented in IQTREE [76]. Calibration points are available in electronic supplementary material, table S2.

(c) Paralog pruning and protein rate of evolution

OG trees were inferred using IQ-TREE as described before, and mulit-copy OGs were decomposed to single-copy using DISCO [77]. We then optimized the branch lengths on the species tree for each decomposed OG using IQ-TREE. Convergent rate analysis was performed with TRACCER [78] on the 20 Branchiopoda species. Gene trees were discarded if they had fewer than three species with or without morphological stasis, or six total, as they were unlikely to be informative. Initially, all Notostraca species were flagged as having the trait of interest (morphological stasis). Subsequently, all Onychocaudata species were flagged as having the trait of interest (morphological disparity). For OGs included in comparative genomic analyses, we tested whether Notostraca have a significant different protein length that might be due to our annotation strategy, fitting a linear mixed model using OGs and species as random effect with the *lmer* function of the lme4 R package [79]. The *p*-value for the fixed effect was computed with the lmerTest R package [80] using the Satterthwaite approach to approximate the number of degrees of freedom.

(d) Gene Ontology-term enrichment analysis

For each OG, GO terms were assigned to the *L. packardi* gene using OMA [81]. When a sequence of that species was missing, another random Notostraca sequence was used. Enrichment analyses were conducted separately for accelerated and decelerated genes using the TopGO R package in Bioconductor [82]. The analyses utilized the Biological Processes ontology and Fisher's exact test with the classic algorithm. GO terms were considered significantly enriched if the *p*-value was less than 0.01. Furthermore, genes with a decelerated rate of protein evolution in Notostraca were further characterized by manually blasting OGs to the NCBI nr dataset. Additionally, we retrieved all genes associated with one of the 5480 GO terms child to 'developmental process' (GO:0032502) and manually assessed how many were either accelerated or decelerated.

(e) Whole-genome alignment and conserved element prediction

Soft-masked genomes resulting from repeat annotation were used to perform a WGA with Progressive Cactus [83], using the previously inferred Notostraca species tree and the long-read-based chromosome-scale genome of *L. packardi* as the reference. Alignment coverage information for each of the six longest scaffolds of *L. packardi*, representing its putative six pseudo-chromosomes [84], was extracted along with a MAF representation of the WGA using cactus-hal2maf. Per-base alignment coverage information was extracted with the halAlignmentDepth program.

A neutral model of evolution was trained with 'halPhyloPTrain.py' on ancestral transposons annotated with RepeatMasker on the reconstructed ancestral genome of Notostraca, using all previously obtained repeat libraries. From this initial neutral model, we separately estimated a conserved and non-conserved model of sequence evolution for each *L. packardi* chromosome using phastCons [44,85] with the parameters: --target-coverage 0.28 --expected-length 30 --estimate-trees. Per-chromosome conserved and non-conserved models were then averaged with PhyloBoot to obtain genome-wide conserved and non-conserved models. These were used in a final PhastCons run with the same target coverage and expected length parameters to obtain discrete CE predictions. Only results obtained from the six *L. packardi* pseudo-chromosomes were used in following analyses. CEs were filtered to remove unalignable genomic regions, defined as genomic positions where fewer than six other Notostraca species could align to the reference genome of *L. packardi*. We excluded all predicted elements in which more than 25% of the positions were covered by unalignable genomic regions.

(f) Gene family expansion and contraction

To calculate the rate of gene family turnover (λ) we used CAFE (v5.1.0; [86]) on the OG counts as inferred by OrthoFinder. Then, after having implemented the CAFE estimation of the gene-family error model, we calculated (i) a global λ for the entire tree, and (ii) two different λs for Notostraca and all the other branchiopods. To test which model better fitted the data, we simulated 100 OG datasets with a λ of 8.56591×10^{-4} and 6,643 simulated families. Then we estimated again a global λ and two different λs for each simulated dataset, in order to compute a distribution of likelihood ratios between the two models. Each CAFE analysis, including simulations, was run for 1000 iterations to ensure convergence of likelihood values. To test whether OGs returned by TRACCER as either accelerated or decelerated in Notostraca also underwent an expansion or contraction of their copy numbers, we employed two different metrics, calculated across all the internal and terminal nodes of Notostraca: (i) the number of significant CAFE expansions and contractions per OG; (ii) the sum of all gene gains and losses per OG. The same metrics were also obtained for accelerated and decelerated genes in Onychocaudata, considering all the internal and terminal nodes of the clade.

Ethics. This work did not require ethical approval from a human subject or animal welfare committee.

Data accessibility. Data and code used for the analyses, as well as intermediate results and a description of provided files, are made available as electronic supplementary materials. Assembled genomes have been submitted to NCBI and are still under processing by the system (submission numbers: SUB15106804, SUB15106571). Genome annotations, together with intermediate results of the analysis and scripts to generate plots, are available from the Dryad Digital Repository [87].

Supplementary material is available online [88].

Declaration of AI use. We have not used AI-assisted technologies in creating this article.

Authors' contributions. G.F.: conceptualization, data curation, formal analysis, visualization, writing—original draft, writing—review and editing; F.N.: conceptualization, data curation, formal analysis, writing—review and editing; J.M.: conceptualization, data curation, formal analysis,

writing—review and editing; C.S.: data curation, formal analysis, writing—review and editing; S.C.: formal analysis, writing—review and editing; F.M.: resources, writing—review and editing; A.L.: funding acquisition, resources, supervision, validation, writing—review and editing.

All authors gave final approval for publication and agreed to be held accountable for the work performed therein.

Conflict of interest declaration. We declare we have no competing interests.

Funding. This work was supported by the Canziani bequest funded to A.L.

Dedication. Authors wish to dedicate the present work to Barbara Mantovani (1956–2025), evolutionary biologist and zoologist. She was a mentor, a colleague, and a friend.

References

1. Simpson GG. 1944 *Tempo and mode in evolution*. New York, NY: Columbia University Press.
2. Barnosky AD. 2001 Distinguishing the effects of the Red Queen and Court Jester on Miocene mammal evolution in the northern Rocky Mountains. *J. Vertebr. Paleontol.* **21**, 172–185. (doi:10.1671/0272-4634(2001)021[0172:DTEOTR]2.0.CO;2)
3. Condamine FL, Rolland J, Höhna S, Sperling FAH, Sanmartín I. 2018 Testing the role of the Red Queen and Court Jester as drivers of the macroevolution of Apollo butterflies. *Syst. Biol*. **67**, 940–964. (doi:10.1093/sysbio/syy009)
4. Berv JS, Field DJ. 2018 Genomic signature of an avian Lilliput effect across the K-Pg Extinction. *Syst. Biol*. **67**, 1–13. (doi:10.1093/sysbio/syx064)
5. Reaney AM, Bouchenak-Khelladi Y, Tobias JA, Abzhanov A. 2020 Ecological and morphological determinants of evolutionary diversification in Darwin's finches and their relatives. *Ecol. Evol*. **10**, 14020–14032. (doi:10.1002/ece3.6994)
6. Patton AH, Harmon LJ, Del Rosario Castañeda M, Frank HK, Donihue CM, Herrel A, Losos JB. 2021 When adaptive radiations collide: different evolutionary trajectories between and within island and mainland lizard clades. *Proc. Natl Acad. Sci. USA* **118**, e2024451118. (doi:10.1073/pnas.2024451118)
7. Li H *et al*. 2024 A double-edged sword: evolutionary novelty along deep-time diversity oscillation in an iconic group of predatory insects (Neuroptera: Mantispoidea). *Syst. Biol.* **74**, 395–420. (doi:10.1093/sysbio/syae068)
8. Kovacs TGL, Walker J, Hellemans S, Bourguignon T, Tatarnic NJ, McRae JM, Ho SYW, Lo N. 2024 Dating in the dark: elevated substitution rates in cave cockroaches (Blattodea: Nocticolidae) have negative impacts on molecular date estimates. *Syst. Biol*. (doi:10.1101/2023.01.17.524483)
9. Iannello M, Forni G, Piccinini G, Xu R, Martelossi J, Ghiselli F, Milani L. 2023 Signatures of extreme longevity: a perspective from bivalve molecular evolution. *Genome Biol. Evol*. **15**, evad159. (doi:10.1093/gbe/evad159)
10. Felice RN, Goswami A. 2018 Developmental origins of mosaic evolution in the avian cranium. *Proc. Natl Acad. Sci. USA* **115**, 555–560. (doi:10.1073/pnas.1716437115)
11. Kin A, Błażejowski B. 2014 The horseshoe crab of the genus *Limulus*: living fossil or stabilomorph? *PLoS One* **9**, e108036. (doi:10.1371/journal.pone.0108036)
12. Cavin L, Guinot G. 2014 Coelacanths as 'almost living fossils'. *Front. Ecol. Evol.* **2**, 49. (doi:10.3389/fevo.2014.00049)
13. Zhou Z, Zheng S. 2003 The missing link in *Ginkgo* evolution. *Nature* **423**, 821–822. (doi:10.1038/423821a)
14. Turner DD. 2019 In defense of living fossils. *Biol. Philos*. **34**, 23. (doi:10.1007/s10539-019-9678-y)
15. Geyer G, Hegna TA, Kelber KP. 2024 The end of the 'living fossil' tale? A new look at Triassic specimens assigned to the tadpole shrimp *Triops cancriformis* (Notostraca) and associated phyllopods from the Vosges region (eastern France). *Pap. Palaeontol*. **10**, e1589. (doi:10.1002/spp2.1589)
16. Amemiya CT *et al*. 2013 The African coelacanth genome provides insights into tetrapod evolution. *Nature* **496**, 311–316. (doi:10.1038/nature12027)
17. Brownstein CD, MacGuigan DJ, Kim D, Orr O, Yang L, David SR, Kreiser B, Near TJ. 2024 The genomic signatures of evolutionary stasis. *Evolution* **78**, 821–834. (doi:10.1093/evolut/qpae028)
18. Korn M, Rabet N, Ghate HV, Marrone F, Hundsdoerfer AK. 2013 Molecular phylogeny of the Notostraca. *Mol. Phylogenetics Evol*. **69**, 1159–1171. (doi:10.1016/j.ympev.2013.08.006)
19. Gueriau P, Rabet N, Clément G, Lagebro L, Vannier J, Briggs DEG, Charbonnier S, Olive S, Béthoux O. 2016 A 365-million-year-old freshwater community reveals morphological and ecological stasis in branchiopod crustaceans. *Curr. Biol*. **26**, 383–390. (doi:10.1016/j.cub.2015.12.039)
20. Luchetti A, Forni G, Martelossi J, Savojardo C, Martelli PL, Casadio R, Skaist AM, Wheelan SJ, Mantovani B. 2021 Comparative genomics of tadpole shrimps (Crustacea, Branchiopoda, Notostraca): dynamic genome evolution against the backdrop of morphological stasis. *Genomics* **113**, 4163–4172. (doi:10.1016/j.ygeno.2021.11.001)
21. Nicolini F, Martelossi J, Forni G, Savojardo C, Mantovani B, Luchetti A. 2023 Comparative genomics of *Hox* and *ParaHox* genes among major lineages of Branchiopoda with emphasis on tadpole shrimps. *Front. Ecol. Evol*. **11**, 23. (doi:10.3389/fevo.2023.1046960)
22. Hay JM, Subramanian S, Millar CD, Mohandesan E, Lambert DM. 2008 Rapid molecular evolution in a living fossil. *Trends Genet*. **24**, 106–109. (doi:10.1016/j.tig.2007.12.002)
23. Savojardo C, Luchetti A, Martelli PL, Casadio R, Mantovani B. 2019 Draft genomes and genomic divergence of two *Lepidurus* tadpole shrimp species (Crustacea, Branchiopoda, Notostraca). *Mol. Ecol. Resour*. **19**, 235–244. (doi:10.1111/1755-0998.12952)
24. Colbourne JK *et al*. 2011 The ecoresponsive genome of *Daphnia pulex*. *Science* **331**, 555–561. (doi:10.1126/science.1197761)
25. Nickel J, Schell T, Holtzem T, Thielsch A, Dennis SR, Schlick-Steiner BC, Cordellier M. 2021 Hybridization dynamics and extensive introgression in the *Daphnia longispina* species complex: new insights from a high-quality *Daphnia galeata* reference genome. *Genome Biol. Evol*. **13**, evab267. (doi:10.1093/gbe/evab267)
26. Byeon E *et al*. 2022 The freshwater water flea *Daphnia magna* NIES strain genome as a resource for CRISPR/Cas9 gene targeting: the glutathione S-transferase omega 2 gene. *Aquat. Toxicol*. **242**, 106021. (doi:10.1016/j.aquatox.2021.106021)
27. Jia J, Dong C, Han M, Ma S, Chen W, Dou J, Liu X. 2022 Multi-omics perspective on studying reproductive biology in *Daphnia sinensis*. *Genomics* **114**, 110309. (doi:10.1016/j.ygeno.2022.110309)
28. Pei Y, Deng Z, Zhang X, Blair D, Hu W, Yin M. 2023 Chromosome-scale genome assembly of the freshwater cladoceran crustacean *Chydorus sphaericus*: a resource for discovery of genes responsive to ecological challenges. *Aquat. Toxicol*. **260**, 106565. (doi:10.1016/j.aquatox.2023.106565)
29. Wersebe MJ, Sherman RE, Jeyasingh PD, Weider LJ. 2023 The roles of recombination and selection in shaping genomic divergence in an incipient ecological species complex. *Mol. Ecol*. **32**, 1478–1496. (doi:10.1111/mec.16383)
30. Baldwin-Brown JG, Weeks SC, Long AD. 2018 A new standard for crustacean genomes: the highly contiguous, annotated genome assembly of the clam shrimp *Eulimnadia texana* reveals *HOX* gene order and identifies the sex chromosome. *Genome Biol. Evol*. **10**, 143–156. (doi:10.1093/gbe/evx280)
31. Simpson JT, Wong K, Jackman SD, Schein JE, Jones SJM, Birol İ. 2009 ABySS: a parallel assembler for short read sequence data. *Genome Res*. **19**, 1117–1123. (doi:10.1101/gr.089532.108)

32. Righetti N, Nicolini F, Forni G, Luchetti A. 2025 Towards a time-tree solution for Branchiopoda diversification: a jackknife assessment of fossil age priors. *Palaeoentomology* **8**, 316–328. (doi:10.11646/palaeoentomology.8.3.8)
33. Sun XY, Xia X, Yang Q. 2016 Dating the origin of the major lineages of Branchiopoda. *Palaeoworld* **25**, 303–317. (doi:10.1016/j.palwor.2015.02.003)
34. Uozumi T, Ishiwata K, Grygier MJ, Sanoamuang LO, Su ZH. 2021 Three nuclear protein-coding genes corroborate a recent phylogenomic model of the Branchiopoda (Crustacea) and provide estimates of the divergence times of the major branchiopodan taxa. *Genes Genet. Syst*. **96**, 13–24. (doi:10.1266/ggs.20-00046)
35. Xu SL, Han BP, Martínez A, Schwentner M, Fontaneto D, Dumont HJ, Kotov AA. 2021 Mitogenomics of Cladocera (Branchiopoda): marked gene order rearrangements and independent predation roots. *Mol. Phylogenetics Evol*. **164**, 107275. (doi:10.1016/j.ympev.2021.107275)
36. Van Damme K, Cornetti L, Fields PD, Ebert D. 2022 Whole-genome phylogenetic reconstruction as a powerful tool to reveal homoplasy and ancient rapid radiation in waterflea evolution. *Syst. Biol*. **71**, 777–787. (doi:10.1093/sysbio/syab094)
37. Bernot JP, Owen CL, Wolfe JM, Meland K, Olesen J, Crandall KA. 2023 Major revisions in pancrustacean phylogeny and evidence of sensitivity to taxon sampling. *Mol. Biol. Evol*. **40**, msad175. (doi:10.1093/molbev/msad175)
38. Wolfe JM, Daley AC, Legg DA, Edgecombe GD. 2016 Fossil calibrations for the arthropod tree of life. *Earth Sci. Rev.* **160**, 43–110. (doi:10.1016/j.earscirev.2016.06.008)
39. Scalzitti N, Jeannin-Girardon A, Collet P, Poch O, Thompson JD. 2020 A benchmark study of *ab initio* gene prediction methods in diverse eukaryotic organisms. *BMC Genom.* **21**, 1–20. (doi:10.1186/s12864-020-6707-9)
40. Weisman CM, Murray AW, Eddy SR. 2022 Mixing genome annotation methods in a comparative analysis inflates the apparent number of lineage-specific genes. *Curr. Biol*. **32**, 2632–2639. (doi:10.1016/j.cub.2022.04.085)
41. Feng S *et al*. 2020 Dense sampling of bird diversity increases power of comparative genomics. *Nature* **587**, 252–258. (doi:10.1038/s41586-020-2873-9)
42. Bejerano G, Pheasant M, Makunin I, Stephen S, Kent WJ, Mattick JS, Haussler D. 2004 Ultraconserved elements in the human genome. *Science* **304**, 1321–1325. (doi:10.1126/science.1098119)
43. Woolfe A *et al*. 2005 Highly conserved non-coding sequences are associated with vertebrate development. *PLoS Biol*. **3**, e7. (doi:10.1371/journal.pbio.0030007)
44. Siepel A *et al*. 2005 Evolutionarily conserved elements in vertebrate, insect, worm, and yeast genomes. *Genome Res*. **15**, 1034–1050. (doi:10.1101/gr.3715005)
45. Long HK, Prescott SL, Wysocka J. 2016 Ever-changing landscapes: transcriptional enhancers in development and evolution. *Cell* **167**, 1170–1187. (doi:10.1016/j.cell.2016.09.018)
46. Andersson R, Sandelin A. 2020 Determinants of enhancer and promoter activities of regulatory elements. *Nat. Rev. Genet*. **21**, 71–87. (doi:10.1038/s41576-019-0173-8)
47. Wong K *et al*. 2021 Divergent enhancer evolution shapes regulatory differences between primates. *Sci. Adv.* **7**, eabc1234. (doi:10.1016/j.cell.2015.08.036)
48. Nguyen DQ, Webber C, Hehir-Kwa J, Pfundt R, Veltman J, Ponting CP. 2008 Reduced purifying selection prevails over positive selection in human copy number variant evolution. *Genome Res*. **18**, 1711–1723. (doi:10.1101/gr.077289.108)
49. Zhang J, Yang JR. 2015 Determinants of the rate of protein sequence evolution. *Nat. Rev. Genet*. **16**, 409–420. (doi:10.1038/nrg3950)
50. Rice AM, McLysaght A. 2017 Dosage sensitivity is a major determinant of human copy number variant pathogenicity. *Nat. Commun*. **8**, 14366. (doi:10.1038/ncomms14366)
51. O'Toole ÁN, Hurst LD, McLysaght A. 2018 Faster evolving primate genes are more likely to duplicate. *Mol. Biol. Evol*. **35**, 107–118. (doi:10.1093/molbev/msx270)
52. Lidgard S, Love AC. 2018 Rethinking living fossils. *Bioscience* **68**, 760–770. (doi:10.1093/biosci/biy084)
53. Wagner P, Haug JT, Sell J, Haug C. 2017 Ontogenetic sequence comparison of extant and fossil tadpole shrimps: no support for the 'living fossil' concept. *PalZ* **91**, 463–472. (doi:10.1007/s12542-017-0370-8)
54. Lindholm M. 2014 Morphologically conservative but physiologically diverse: the mode of stasis in Anostraca (Crustacea: Branchiopoda). *Evol. Biol*. **41**, 503–507. (doi:10.1007/s11692-014-9283-6)
55. Casane D, Laurenti P. 2013 Why coelacanths are not 'living fossils? A review of molecular and morphological data. *Bioessays* **35**, 332–338. (doi:10.1002/bies.201200145)
56. Lamichhaney S *et al*. 2015 Evolution of Darwin's finches and their beaks revealed by genome sequencing. *Nature* **518**, 371–375. (doi:10.1038/nature14181)
57. Carroll SB. 2008 Evo-devo and an expanding evolutionary synthesis: a genetic theory of morphological evolution. *Cell* **134**, 25–36. (doi:10.1016/j.cell.2008.06.030)
58. Van Belleghem SM *et al*. 2017 Complex modular architecture around a simple toolkit of wing pattern genes. *Nat. Ecol. Evol*. **1**, 52. (doi:10.1038/s41559-016-0052)
59. Marrone F, Alonso M, Pieri V, Agugliaro C, Stoch F. 2015 The crustacean fauna of Bayan Onjuul area (Tôv Province, Mongolia) (Crustacea: Branchiopoda, Copepoda, Ostracoda). *Nort West. J. Zool.* **11**, 288–295.
60. Marrone F, Korn M, Stoch F, Naselli-Flores L, Turki S. 2016 Updated checklist and distribution of large branchiopods (Branchiopoda: Anostraca, Notostraca, Spinicaudata) in Tunisia. *Biogeographia* **31**, B631132736. (doi:10.21426/B631132736)
61. Bolger AM, Lohse M, Usadel B. 2014 Trimmomatic: a flexible trimmer for Illumina sequence data. *Bioinformatics* **30**, 2114–2120. (doi:10.1093/bioinformatics/btu170)
62. Pryszcz LP, Gabaldón T. 2016 Redundans: an assembly pipeline for highly heterozygous genomes. *Nucleic Acids Res*. **44**, e113–e113. (doi:10.1093/nar/gkw294)
63. Challis R, Richards E, Rajan J, Cochrane G, Blaxter M. 2020 BlobToolKit—interactive quality assessment of genome assemblies. *G3* **10**, 1361–1374. (doi:10.1534/g3.119.400908)
64. Li H. 2018 Minimap2: pairwise alignment for nucleotide sequences. *Bioinformatics* **34**, 3094–3100. (doi:10.1093/bioinformatics/bty191)
65. Manni M, Berkeley MR, Seppey M, Simão FA, Zdobnov EM. 2021 BUSCO update: novel and streamlined workflows along with broader and deeper phylogenetic coverage for scoring of eukaryotic, prokaryotic, and viral genomes. *Mol. Biol. Evol*. **38**, 4647–4654. (doi:10.1093/molbev/msab199)
66. Flynn JM, Hubley R, Goubert C, Rosen J, Clark AG, Feschotte C, Smit AF. 2020 RepeatModeler2 for automated genomic discovery of transposable element families. *Proc. Natl Acad. Sci. USA* **117**, 9451–9457. (doi:10.1073/pnas.1921046117)
67. Orozco-Arias S, Sierra P, Durbin R, González JM. 2023 MCHelper automatically curates transposable element libraries across eukaryotic species. *bioRxiv*2023.10.17.562682. (doi:10.1101/2023.10.17.562682)
68. Tarailo-Graovac M, Chen N. 2009 Using RepeatMasker to identify repetitive elements in genomic sequences. *Curr. Protoc. Bioinform*. **25**, 4.10.1-4.10.14. (doi:10.1002/0471250953.bi0410s25)
69. Stanke M, Keller O, Gunduz I, Hayes A, Waack S, Morgenstern B. 2006 AUGUSTUS: *ab initio* prediction of alternative transcripts. *Nucleic Acids Res*. **34**, W435–W439. (doi:10.1093/nar/gkl200)
70. Emms DM, Kelly S. 2019 OrthoFinder: phylogenetic orthology inference for comparative genomics. *Genome Biol*. **20**, 238. (doi:10.1186/s13059-019-1832-y)
71. Katoh K, Kuma KI, Toh H, Miyata T. 2005 MAFFT version 5: improvement in accuracy of multiple sequence alignment. *Nucleic Acids Res*. **33**, 511–518. (doi:10.1093/nar/gki198)
72. Capella-Gutiérrez S, Silla-Martínez JM, Gabaldón T. 2009 trimAl: a tool for automated alignment trimming in large-scale phylogenetic analyses. *Bioinformatics* **25**, 1972–1973. (doi:10.1093/bioinformatics/btp348)
73. Nguyen LT, Schmidt HA, von Haeseler A, Minh BQ. 2015 IQ-TREE: a fast and effective stochastic algorithm for estimating maximum-likelihood phylogenies. *Mol. Biol. Evol*. **32**, 268–274. (doi:10.1093/molbev/msu300)

74. Kalyaanamoorthy S, Minh BQ, Wong TKF, von Haeseler A, Jermiin LS. 2017 ModelFinder: fast model selection for accurate phylogenetic estimates. *Nat. Methods* **14**, 587–589. (doi:10.1038/nmeth.4285)
75. Hoang DT, Chernomor O, von Haeseler A, Minh BQ, Vinh LS. 2018 UFBoot2: improving the ultrafast bootstrap approximation. *Mol. Biol. Evol*. **35**, 518–522. (doi:10.1093/molbev/msx281)
76. To TH, Jung M, Lycett S, Gascuel O. 2016 Fast dating using least-squares criteria and algorithms. *Syst. Biol*. **65**, 82–97. (doi:10.1093/sysbio/syv068)
77. Willson J, Roddur MS, Liu B, Zaharias P, Warnow T. 2022 DISCO: species tree inference using multicopy gene family tree decomposition. *Syst. Biol*. **71**, 610–629. (doi:10.1093/sysbio/syab070)
78. Treaster S, Daane JM, Harris MP. 2021 Refining convergent rate analysis with topology in mammalian longevity and marine transitions. *Mol. Biol. Evol*. **38**, 5190–5203. (doi:10.1093/molbev/msab226)
79. Bates D, Mächler M, Bolker B, Walker S. 2015 Fitting linear mixed-effects models using lme4. *J. Stat. Softw.* **67**, 1–48. (doi:10.18637/jss.v067.i01)
80. Kuznetsova A, Brockhoff PB, Christensen RHB. 2017 lmerTest package: tests in linear mixed effects models. *J. Stat. Softw.* **82**, 1–26. (doi:10.18637/jss.v082.i13)
81. Altenhoff AM *et al*. 2024 OMA orthology in 2024: improved prokaryote coverage, ancestral and extant GO enrichment, a revamped synteny viewer and more in the OMA Ecosystem. *Nucleic Acids Res*. **52**, D513–D521. (doi:10.1093/nar/gkad1020)
82. Alexa A, Rahnenfuhrer J. 2024 topGO: Enrichment Analysis for Gene Ontology (R package version 2.56.0). (doi:10.18129/B9.bioc.topGO). See https://bioconductor.org/packages/topGO.
83. Armstrong J *et al*. 2020 Progressive Cactus is a multiple-genome aligner for the thousand-genome era. *Nature* **587**, 246–251. (doi:10.1038/s41586-020-2871-y)
84. Kieran Blair SR, Hull J, Escalona M, Finger A, Joslin SE, Sahasrabudhe R, Schreier A. 2022 The reference genome of the vernal pool tadpole shrimp, *Lepidurus packardi*. *J. Hered*. **113**, 706–711. (doi:10.1093/jhered/esac051)
85. Hubisz MJ, Pollard KS, Siepel A. 2011 PHAST and RPHAST: phylogenetic analysis with space/time models. *Brief. Bioinformatics* **12**, 41–51. (doi:10.1093/bib/bbq072)
86. Mendes FK, Vanderpool D, Fulton B, Hahn MW. 2020 CAFE 5 models variation in evolutionary rates among gene families. *Bioinformatics* **36**, 5516–5518. (doi:10.1093/bioinformatics/btaa1022)
87. Forni G, Nicolini F, Martelossi J, Savojardo C, Corneti S, Marrone F, Luchetti A. 2025 Data from: The elusive genomic signature of tadpole shrimps' ancient morphology [Data and code]. Dryad Digital Repository. (doi:10.5061/dryad.cz8w9gjh1)
88. Forni G, Nicolini F, Martelossi J, Savojardo C, Corneti S, Marrone F *et al*. 2026 Supplementary material from: The elusive genomic signature of tadpole shrimps' ancient morphology. Figshare. (doi:10.6084/m9.figshare.c.8292155)